Centrum Wiskunde & Informatica

Computational Challenges in Photoacoustic and Ultrasonic Breast Imaging

Jiri Jaros, Felix Lucka

Excalibur SLE Workshop on Inverse Problems and Optimisation
7th May 2021

Quantitative Photoacoustic Breast Imaging

- hybrid imaging: "light in, sound out"
- non-ionizing, near-infrared radiation
- quantitative images of optical properties
- novel diagnostic information

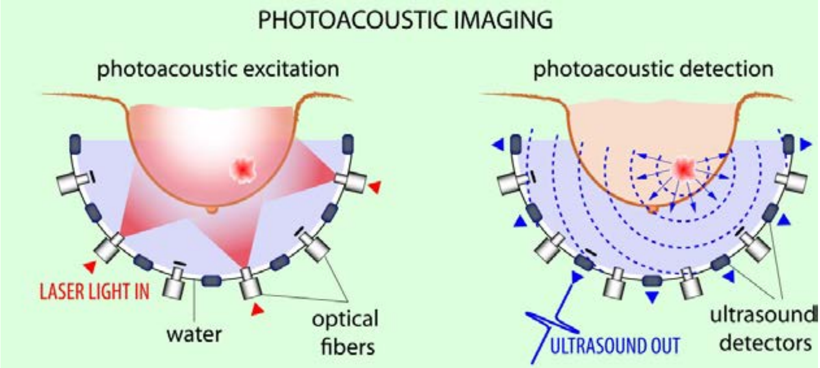

Photoacoustic Imaging: Spectral Properties

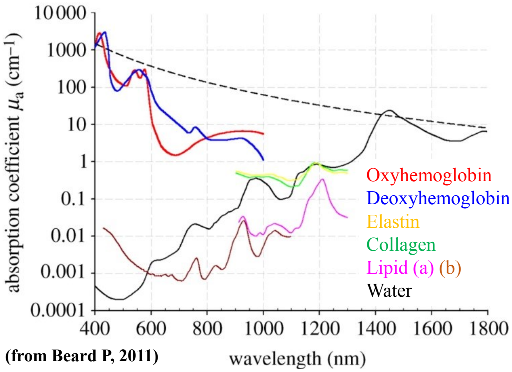

(from Beard P, 2011)

- different wavelengths allow quantitative spectroscopic examinations.
- gap between oxygenated and deoxygenated blood.
- use of contrast agents for molecular imaging.

Quantitative Ultrasonic Breast Imaging

- "sound in, sound out"
- different from conventional US but as safe
- quantitative images of acoustic properties
- novel diagnostic information

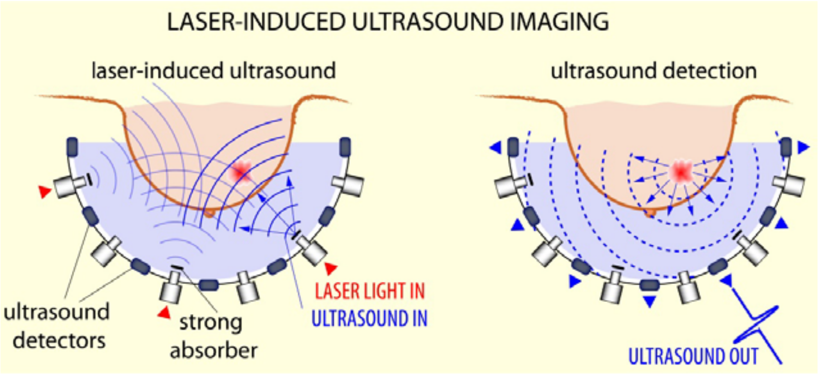

Partners in H2020 Project

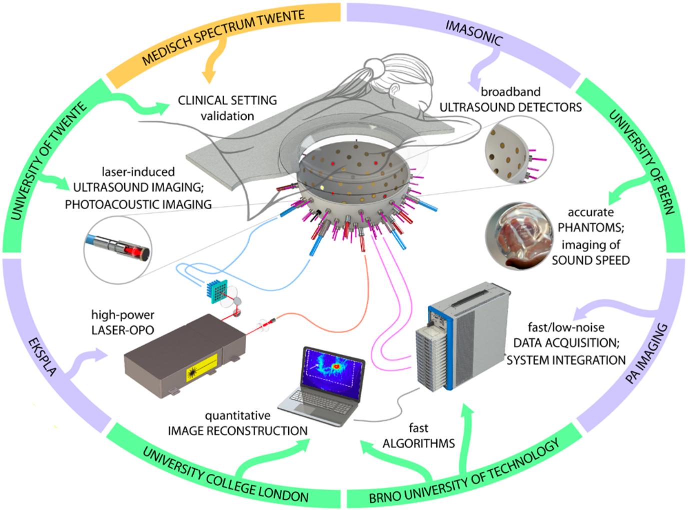

Aim: novel diagnostic information from high resolution maps of optical and acoustic properties

Our Contributions

simulation studies for

- ultrasonic transducer specification
- light excitation design
- sensing pattern design
- measurement protocol design

reconstruction algorithm design:

- accuracy vs. computational time/resources/complexity
- scanner modelling
- assist high performance computing implementation

assist **phantom & calibration design**

process data, refine measurement procedures

Mathematical Modelling (simplified)

Quantitative Photoacoustic Tomography (QPAT)

radiative transfer equation (RTE) + acoustic wave equation

$$(v \cdot \nabla + \mu_a(x) + \mu_s(x))\, \phi(x, v) = q(x, v) + \mu_s(x) \int \Theta(v, v')\phi(x, v')dv',$$

$$p^{PA}(x, t = 0) = p_0 := \Gamma(x)\mu_a(x) \int \phi(x, v)dv, \qquad \partial_t p^{PA}(x, t = 0) = 0$$

$$(c(x)^{-2}\partial_t^2 - \Delta)p^{PA}(x, t) = 0, \qquad f^{PA} = Mp^{PA}$$

Ultrasound Tomography (UST)

$$(c(x)^{-2}\partial_t^2 - \Delta)p_i^{US}(x, t) = s_i(x, t), \qquad f_i^{US} = M_i p_i^{US}, \qquad i = 1, \dots, n_s$$

Step-by-step inversion

1. $f^{US} \to c$: acoustic parameter identification from boundary data.
2. $f^{PA} \to p_0$: acoustic initial value problem with boundary data.
3. $p_0 \to \mu_a$: optical parameter identification from internal data.

Reconstruction of Initial Photoacoustic Pressure

$$(c(x)^{-2}\partial_t^2 - \Delta)p^{PA}(x,t) = 0, \quad p^{PA}(x, t=0) = p_0, \quad f^{PA} = Mp^{PA}$$

$$f^{PA} = MAp_0$$

$$\hat{p}_0 = \operatorname*{argmin}_{p_0 \in \mathcal{C}} \left\| MAp_0 - f^{PA} \right\|_W^2 + \mathcal{R}(p_0)$$

- ✓ linear inverse problem
- ✓ variational approach
- ✓ first order optimization with early stopping
- ! model acoustic properties, model discrepancies
- ! model /calibrate piezoelectric sensor properties: sensitivity, impulse response, angular sensitivity, ...
- ! parameter choices, image artifacts,...
- ! numerical wave simulations: broadband up to $\geqslant 1.5$MHz, $\leqslant 0.5$mm

Acoustic Wave Propagation: Numerical Solution

- **Direct methods**, such as finite-difference, pseudospectral, finite/spectral element, discontinous Galerkin.
- **Integral equation methods**, e.g. boundary element
- **Asymptotic methods**, e.g., geometrical optics, Gaussian beams

Acoustic Wave Propagation: Numerical Solution

- Direct methods, such as finite-difference, **pseudospectral**, finite/spectral element, discontinous Galerkin.
- Integral wave equation methods, e.g. boundary element.
- Asymptotic methods, e.g., geometrical optics, Gaussian beams.

k-Wave: *k*-space pseudospectral method solving the underlying system of first order conservation laws.

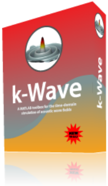

- Compute spatial derivatives in Fourier space: 3D FFTs.
- Parallel/GPU computing leads to massive speed-ups.
- Modify finite temporal differences by *k*-space operator and use staggered grids for accuracy and robustness.
- Perfectly matched layer to simulate free-space propagation.

B. Treeby and B. Cox, 2010. k-Wave: MATLAB toolbox for the simulation and reconstruction of photoacoustic wave fields, *Journal of Biomedical Optics.*

Healthy volunteer, 797nm, baseline

$$\hat{p}_0 = \operatorname{argmin}_{p_0 \geqslant 0} \left\| MAp_0 - f^{PA} \right\|_W^2$$

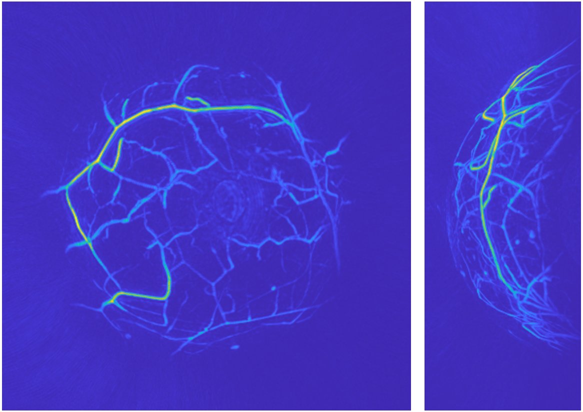

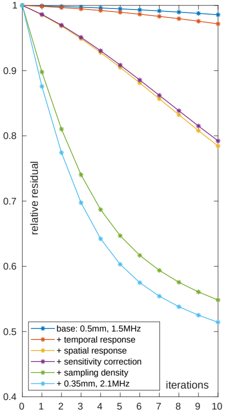

single wave simulation on 0.50mm: 2min 20; 10 iterations: 1h 20min

Healthy volunteer, 797nm, add impulse response

$$\hat{p}_0 = \mathrm{argmin}_{p_0 \geqslant 0} \left\| M A p_0 - f^{PA} \right\|_W^2$$

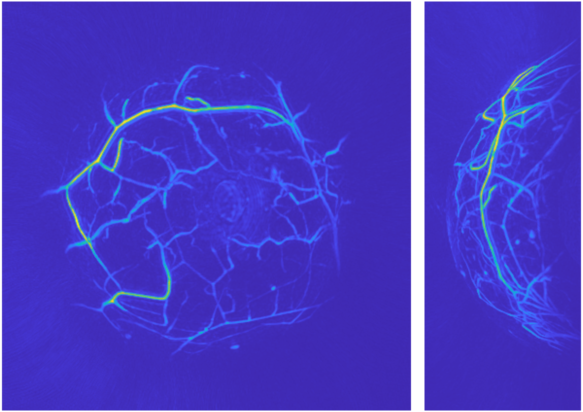

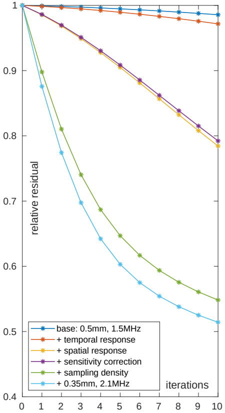

single wave simulation on 0.50mm: 2min 20; 10 iterations: 1h 20min

Healthy volunteer, 797nm, add spatial response

$$\hat{p}_0 = \mathrm{argmin}_{p_0 \geqslant 0} \left\| M A p_0 - f^{PA} \right\|_W^2$$

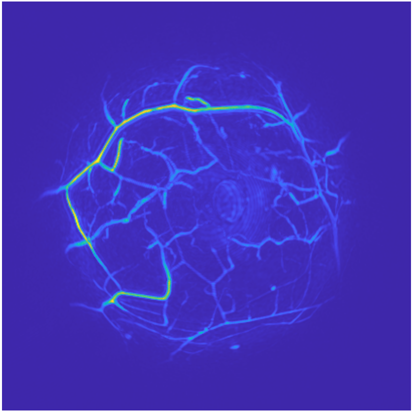

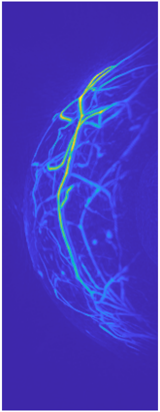

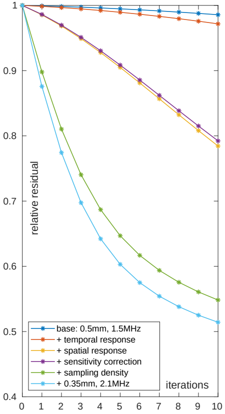

single wave simulation on 0.50mm: 2min 20; 10 iterations: 1h 20min

Healthy volunteer, 797nm, add sensitivity

$$\hat{p}_0 = \operatorname{argmin}_{p_0 \geqslant 0} \left\| MAp_0 - f^{PA} \right\|_W^2$$

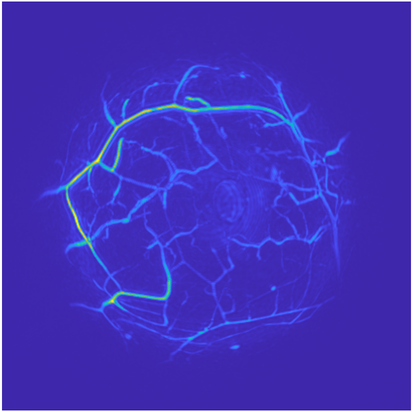

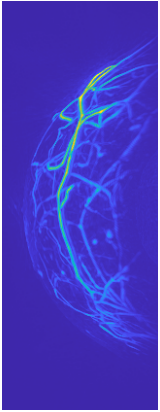

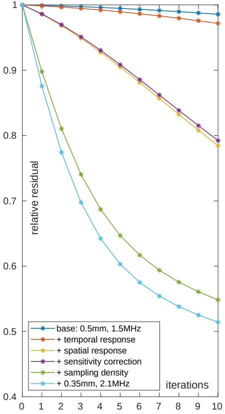

single wave simulation on 0.50mm: 2min 20; 10 iterations: 1h 20min

Healthy volunteer, 797nm, add sampling density

$$\hat{p}_0 = \operatorname{argmin}_{p_0 \geqslant 0} \left\| M A p_0 - f^{PA} \right\|_W^2$$

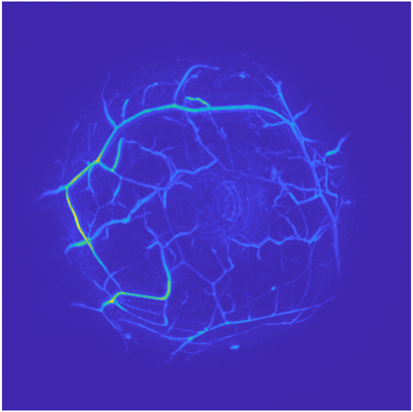

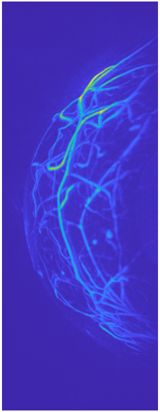

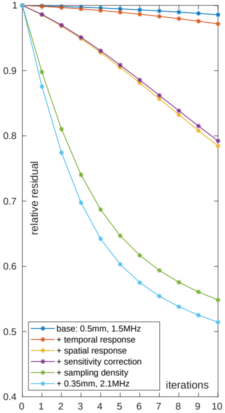

single wave simulation on 0.50mm: 2min 20; 10 iterations: 1h 20min

Healthy volunteer, 797nm, increase resolution/bandwidth

$$\hat{p}_0 = \mathrm{argmin}_{p_0 \geqslant 0} \left\| M A p_0 - f^{PA} \right\|_W^2$$

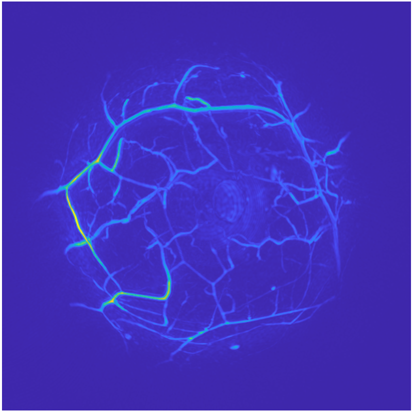

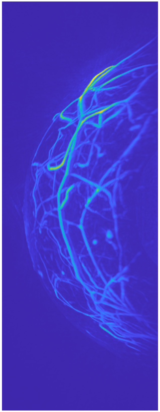

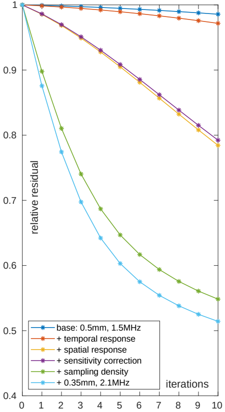

single wave simulation on 0.35mm: 12min 10; 10 iterations: 4h 8min

Healthy volunteer, 720nm

$p_0 = \Gamma(x)\,\mu_a(x,\lambda)\,\Phi(x,\lambda,\mu_a)$

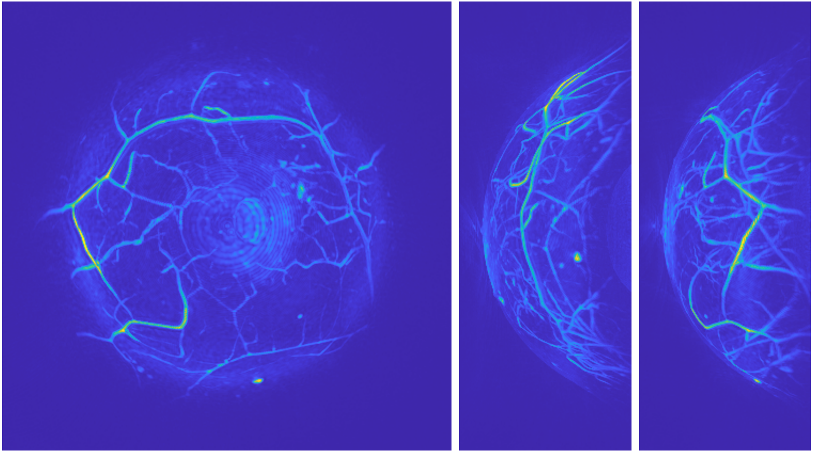

Healthy volunteer, 890nm

$p_0 = \Gamma(x)\,\mu_a(x,\lambda)\,\Phi(x,\lambda,\mu_a)$

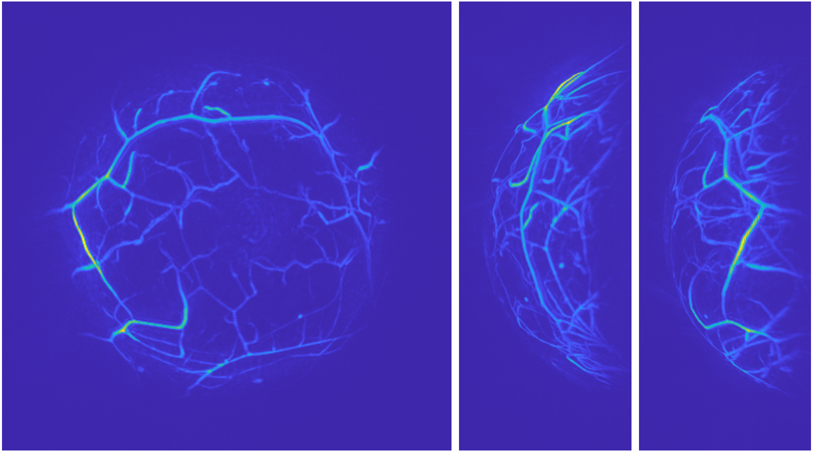

Spectral dimension: ratio images 890nm / 720nm

$p_0 = \Gamma(x)\,\mu_a(x,\lambda)\,\Phi(x,\lambda,\mu_a)$

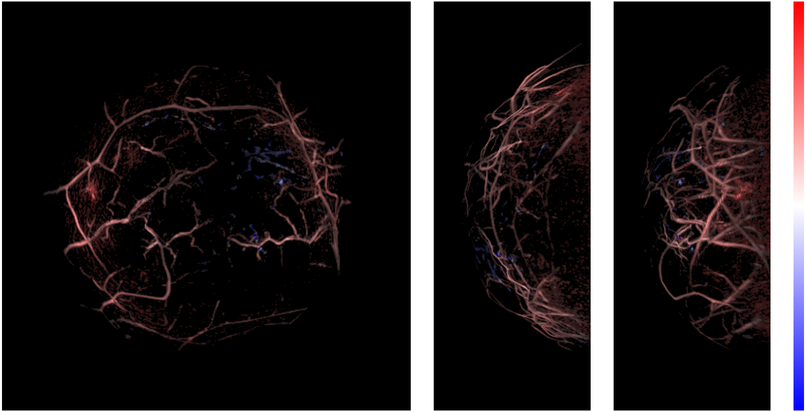

initial pressure corrected with background fluence, thresholded by intensity and only structures 1-20mm are shown; shown is logarithm of ratio; blue = relative decrease (ratio < 1), white = no change (ratio $= 1$), red = relative increase (ratio > 1)

Optical & Spectral Inversion: Overview

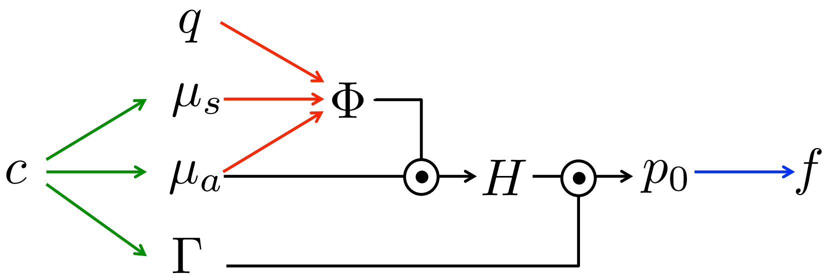

- mapping from c to (μ_a, μ_s, Γ): spectra?
- q: light source properties?
- mapping from (μ_a, μ_s, q) to Φ: non-linear.

The RTE and Toast++

Radiative transfer equation

$$(v \cdot \nabla + \mu_a(x) + \mu_s(x))\,\phi(x,v) = q(x,v) + \mu_s(x) \int \Theta(v,v')\phi(x,v')dv'$$

$$\Phi(x) = \int \phi(x,v)dv,$$ **!** $(x,v) \in \mathbb{R}^5 \rightsquigarrow$ direct FEM infeasible.

Diffusion approximation

$$(\mu_a(x) - \nabla \cdot \kappa(x)\nabla)\,\Phi(x) = \int q(x,v)dv, \quad \kappa = \frac{1}{\nu(\mu_a + \mu_s(1-g))}$$

source modelling? diffusivity matching?

Schweiger, Arridge, 2014. The Toast++ software suite for forward and inverse modeling in optical tomography, *Journal of Biomedical Optics.*

Macdonald, Arridge, Powell, 2020. Efficient inversion strategies for estimating optical properties with Monte Carlo radiative transport models, *Journal of Biomedical Optics.*

Model Based Inversion

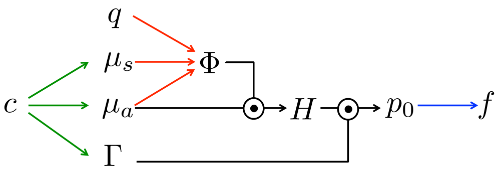

$$\hat{c} = \underset{c \in \mathcal{C}}{\operatorname{argmin}} \sum_{\lambda=1}^{N_\lambda} \int_{ROI} \left(p_{0,\lambda}^{recon} - p_{0,\lambda}(c)\right)^2 dx$$

- solve via iterative first order method (L-BFGS)
- derivatives of $\Phi(\mu_a, \mu_s)$ via adjoint method: two solves of light model per iteration (per wavelength).
- grid/mesh interpolation

Malone, Powell, Cox, Arridge, 2015. Reconstruction-classification method for quantitative photoacoustic tomography, *JBO*.

We Have Done This Before?

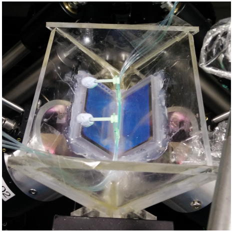 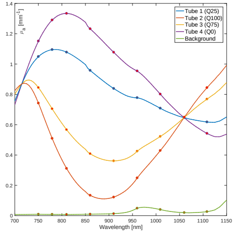

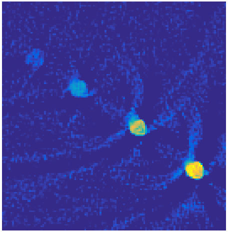

- well-controlled laboratory experiment
- full characterization of optical, acoustic and thermoelastic properties of phantom (sO_2 analogue)
- examined sensitivities, computational aspects, etc.
- promising results but a lot to improve

Fonseca, Malone, L, Ellwood, An, Arridge, Beard, Cox, 2017. Three-dimensional photoacoustic imaging and inversion for accurate quantification of chromophore distributions, *Proc. SPIE 2017.*

UST Reconstruction Approaches

$$(c(x)^{-2}\partial_t^2 - \Delta)p_i^{US}(x,t) = s_i(x,t), \qquad f_i^{US} = M_i p_i^{US} \qquad i = 1, \dots, n_{src}$$

Travel time tomography: geometrical optics approximation.

- ✓ robust & computationally efficient
- ! valid for high frequencies (attenuation!), low res, lots of data

Full waveform inversion (FWI): fit full wave model to all data.

- ✓ high res from little data, transducer modelling, constraints
- ! many wave simulations, complex numerical optimization
- • low TRL but already used in 2D systems

Javaherian, L, Cox, 2020. Refraction-corrected ray-based inversion for three-dimensional ultrasound tomography of the breast, *Inverse Problems.*

Time Domain Full Waveform Inversion

$$F(c)p_i := (c^{-2}\partial_t^2 - \Delta)p_i = s_i, \qquad f_i = M_i\, p_i, \quad i = 1, \dots, n_{src}$$

$$\min_{c \in \mathcal{C}} \sum_i^{n_{src}} \mathcal{D}\left(f_i(c), f_i^\delta\right) \quad s.t. \quad f_i(c) = M_i F^{-1}(c) s_i$$

gradient for **first-order optimization** via **adjoint state method**:

$$\nabla_c \mathcal{D}\left(f(c), f^\delta\right) = 2\int_0^T \frac{1}{c(x)^3}\left(\frac{\partial^2 p(x,t)}{\partial t^2}\right) q^*(x,t) \quad ,$$

where $(c^{-2}\partial_t^2 - \Delta)q^* = s^*$, $s^*(x,t)$ is time-reversed data discrepancy

$\rightarrow$ **two wave simulations for one gradient**

Starting point in 2D:

Pérez-Liva, Herraiz, Udías, Miller, Cox, Treeby 2017. Time domain reconstruction of sound speed and attenuation in ultrasound computed tomography using full wave inversion, *JASA.*

3D Time Domain FWI for Breast UST

$$\min_{c \in \mathcal{C}} \sum_{i}^{n_{src}} \mathcal{D}\left(M_i F^{-1}(c) s_i, f_i^{\delta}\right)$$

$$\nabla_c \mathcal{D}\left(f(c), f^{\delta}\right) = 2 \int_0^T \frac{1}{c(x)^3} \left(\frac{\partial^2 p(x,t)}{\partial t^2}\right) q^*(x,t)$$

Challenges and solutions for 3D:

- **!** 2 x n_{src} wave simulations per gradient
- **!** computationally & stochastically efficient gradient estimator
- **!** memory requirements of gradient computation
- **!** slow convergence and local minima
- **!** computational resources

3D Time Domain FWI for Breast UST

$$\min_{c \in \mathcal{C}} \sum_{i}^{n_{src}} \mathcal{D}\left(M_i F^{-1}(c) s_i, f_i^{\delta}\right)$$

$$\nabla_c \mathcal{D}\left(f(c), f^{\delta}\right) = 2 \int_0^T \frac{1}{c(x)^3} \left(\frac{\partial^2 p(x,t)}{\partial t^2}\right) q^*(x,t)$$

Challenges and solutions for 3D:

! 2 x n_{src} wave simulations per gradient
$\longrightarrow$ **stochastic quasi-newton optimization (SL-BFGS)**

! computationally & stochastically efficient gradient estimator

! memory requirements of gradient computation

! slow convergence and local minima

! computational resources

3D Time Domain FWI for Breast UST

$$\min_{c\in\mathcal{C}} \sum_{i}^{n_{src}} \mathcal{D}\left(M_i F^{-1}(c) s_i, f_i^{\delta}\right)$$

$$\nabla_c \mathcal{D}\left(f(c), f^{\delta}\right) = 2\int_0^T \frac{1}{c(x)^3}\left(\frac{\partial^2 p(x,t)}{\partial t^2}\right) q^*(x,t)$$

Challenges and solutions for 3D:

! 2 x n_{src} wave simulations per gradient
$\longrightarrow$ **stochastic quasi-newton optimization (SL-BFGS)**

! computationally & stochastically efficient gradient estimator
$\longrightarrow$ **source encoding for time-invariant systems**

! memory requirements of gradient computation

! slow convergence and local minima

! computational resources

3D Time Domain FWI for Breast UST

$$\min_{c \in \mathcal{C}} \sum_{i}^{n_{src}} \mathcal{D}\left(M_i F^{-1}(c) s_i, f_i^\delta\right)$$

$$\nabla_c \mathcal{D}\left(f(c), f^\delta\right) = 2 \int_0^T \frac{1}{c(x)^3} \left(\frac{\partial^2 p(x,t)}{\partial t^2}\right) q^*(x,t)$$

Challenges and solutions for 3D:

! 2 x n_{src} wave simulations per gradient
$\longrightarrow$ **stochastic quasi-newton optimization (SL-BFGS)**

! computationally & stochastically efficient gradient estimator
$\longrightarrow$ **source encoding for time-invariant systems**

! memory requirements of gradient computation
$\longrightarrow$ **time-reversal based gradient computation**

! slow convergence and local minima

! computational resources

3D Time Domain FWI for Breast UST

$$\min_{c \in \mathcal{C}} \sum_{i}^{n_{src}} \mathcal{D}\left(M_i F^{-1}(c) s_i, f_i^{\delta}\right)$$

$$\nabla_c \mathcal{D}\left(f(c), f^{\delta}\right) = 2 \int_0^T \frac{1}{c(x)^3} \left(\frac{\partial^2 p(x,t)}{\partial t^2}\right) q^*(x,t)$$

Challenges and solutions for 3D:

- ! 2 x n_{src} wave simulations per gradient
  $\longrightarrow$ **stochastic quasi-newton optimization (SL-BFGS)**
- ! computationally & stochastically efficient gradient estimator
  $\longrightarrow$ **source encoding for time-invariant systems**
- ! memory requirements of gradient computation
  $\longrightarrow$ **time-reversal based gradient computation**
- ! slow convergence and local minima
  $\longrightarrow$ **coarse-to-fine multigrid schemes**
- ! computational resources

3D Time Domain FWI for Breast UST

$$\min_{c \in \mathcal{C}} \sum_{i}^{n_{src}} \mathcal{D}\left(M_i F^{-1}(c) s_i, f_i^{\delta}\right)$$

$$\nabla_c \mathcal{D}\left(f(c), f^{\delta}\right) = 2 \int_0^T \frac{1}{c(x)^3} \left(\frac{\partial^2 p(x,t)}{\partial t^2}\right) q^*(x,t)$$

Challenges and solutions for 3D:

- **!** 2 x n_{src} wave simulations per gradient
  $\longrightarrow$ **stochastic quasi-newton optimization (SL-BFGS)**
- **!** computationally & stochastically efficient gradient estimator
  $\longrightarrow$ **source encoding for time-invariant systems**
- **!** memory requirements of gradient computation
  $\longrightarrow$ **time-reversal based gradient computation**
- **!** slow convergence and local minima
  $\longrightarrow$ **coarse-to-fine multigrid schemes**
- **!** computational resources
  $\longrightarrow$ **runs on single GPU, can utilize multiple GPUs**

3D FWI: Setup

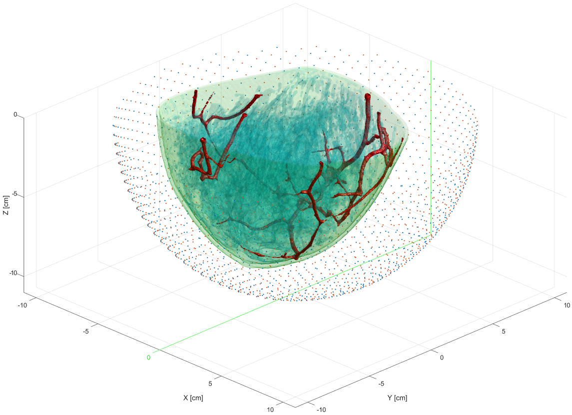

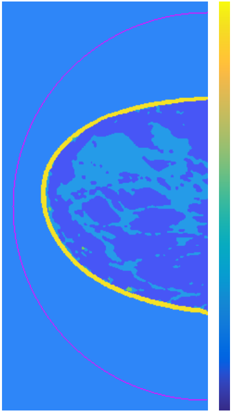

- color range 1435-1665 m/s
- 3D breast phantom at 0.5mm resolution, 1024 sources and receivers
- $442 \times 442 \times 222$ voxel, 3912 time steps

Yang Lou et al. Generation of anatomically realistic numerical phantoms for photoacoustic and ultrasonic breast imaging, *JBO, 2017.*

Starting point in 24h on desktop with single GPU

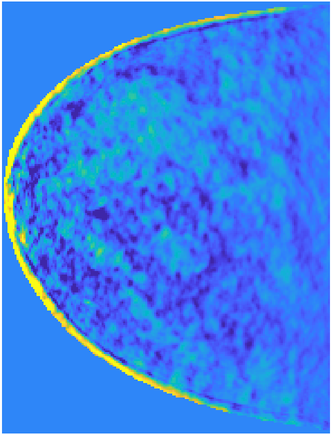

color range 1435 to 1665 m/s

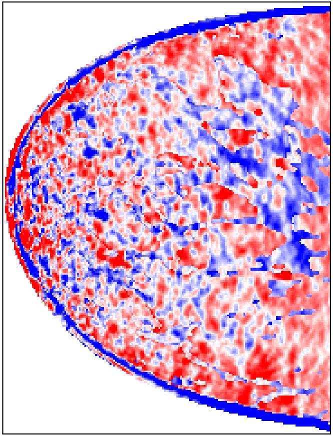

color range -50 to +50 m/s

- single grid
- SGD
- normal single source gradient estimator

3D FWI in 24h on desktop with single GPU

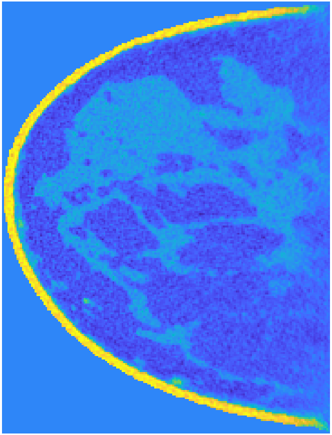

color range 1435 to 1665 m/s

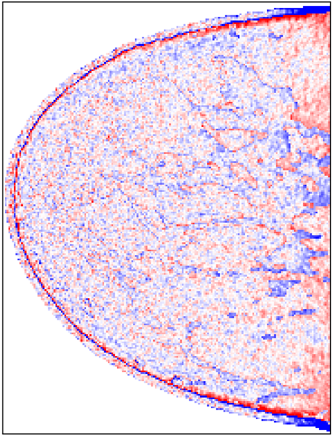

color range -50 to +50 m/s

- multi-grid with 3 level, coarsening factor 2
- SL-BFGS, slowness transform, prog. iter averaging
- time-reversal based source encoding gradient estimator

3D FWI in 24h on cluster with 4 GPU

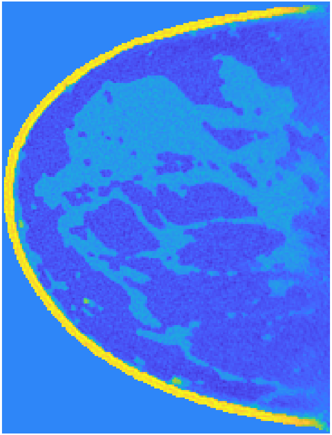

color range 1435 to 1665 m/s

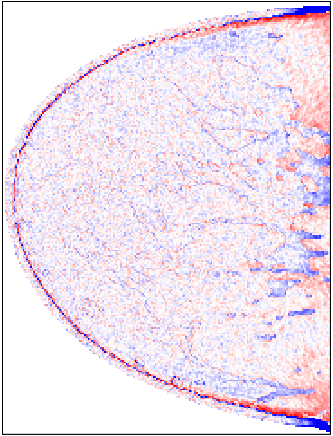

color range -50 to +50 m/s

- multi-grid with 3 level, coarsening factor 2
- SL-BFGS, slowness transform, prog. iter averaging
- time-reversal based source encoding gradient estimator

3D FWI in 24h on cluster with 16 GPU

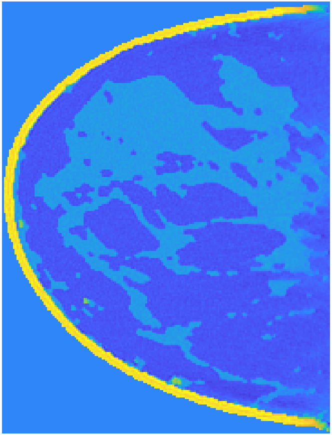

color range 1435 to 1665 m/s

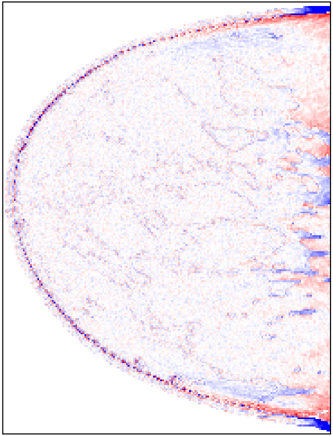

color range -50 to +50 m/s

- multi-grid with 3 level, coarsening factor 2
- SL-BFGS, slowness transform, prog. iter averaging
- time-reversal based source encoding gradient estimator

Summary

- novel diagnostic information from optical and acoustic properties
- 3D, high res, quantitative, deep into the breast
- 5 years of design, specification, component improvement
- patient study under way
- three large-scale inverse problems
- linear and non-linear
- wave equation and photon transport
- model calibrations, approximations
- integration into clinical trajectories?
- computations are significant bottleneck

L, Pérez-Liva, Treeby, Cox, 2021. High Resolution 3D Ultrasonic Breast Imaging by Time-Domain Full Waveform Inversion, *arXiv:2102.00755.*

Fonseca, Malone, L, Ellwood, An, Arridge, Beard, Cox, 2017. Three-dimensional photoacoustic imaging and inversion for accurate quantification of chromophore distributions, *Proc. SPIE 2017.*

Thank you for your attention!

- **L, Pérez-Liva, Treeby, Cox, 2021.** High Resolution 3D Ultrasonic Breast Imaging by Time-Domain Full Waveform Inversion, *arXiv:2102.00755.*
- **Fonseca, Malone, L, Ellwood, An, Arridge, Beard, Cox, 2017.** Three-dimensional photoacoustic imaging and inversion for accurate quantification of chromophore distributions, *Proc. SPIE 2017.*